Journal of Japan Association for Earthquake Engineering, Vol. 18, No. 3, 2018

LIQUEFACTION DAMAGE REDUCTION MEASURES FOR SMALL-SCALE STRUCTURES BY GRAVEL REPLACEMENT UNDER THE OUTER CIRCUMFERENCE OF THE STRUCTURE

Hideyuki MANO[1], Yasuhiro SHAMOTO[2], Akira ISHIKAWA[3] and Katsumi YOSHINARI[4]

[1] Manager, Construction Technology Department, Shimizu Corporation, Tokyo, Japan,
mano_h@shimz.co.jp
[2] Retiree (Former Research Fellow, Shimizu Corporation)

[3] Senior Research Engineer, Institute of Technology Shimizu Corporation, Tokyo, Japan,
akira.ishikawa@shimz.co.jp
[4] Institute of Technology Shimizu Corporation, Tokyo, Japan,
yoshin@shimz.co.jp

ABSTRACT: A new liquefaction countermeasure for small structures was proposed to reduce liquefaction damage. In our approach, the ground below the perimeter of the foundation circumference is replaced by gravel, opening a drainage route to the ground surface. Centrifugal model tests confirmed the effectiveness of the proposed method. The method does not prevent liquefaction, but significantly reduces the degree of tilting of the structures.

Key Words: Liquefaction, Progressive failure, Centrifugal model test, Drainage

1. INTRODUCTION

The 2011 off the Pacific coast of Tohoku Earthquake produced major damage due to liquefaction, mainly in reclaimed land in Tokyo Bay area and in the river basins of the Kanto region[1)]. A great deal of money and time was required for restoration. In the southern part of the Kanto region, the seismic intensity did not exceed upper 5 on the Japanese scale of 7, so damage to buildings supported by piles was relatively small. However, small-scale structures, external structures, and infrastructures such as roads, water supplies, and sewer systems, which were not subject to liquefaction countermeasures, suffered significant liquefaction damage. These small-scale structures deliver raw materials, electricity, water, information, and so forth. If these facilities are damaged, even if the main building is not damaged, it will cause serious interruptions to business continuity. Conventional countermeasures against liquefaction have involved increasing the density of the ground[2)], suppressing ground shear deformation[3)], or supporting the structure with piles. However, these measures must be applied to the entire liquefiable layer, and the associated cost has deterred application to small-scale structures. In the

wake of The Tohoku Earthquake, some studies on liquefaction damage mitigation methods for small-scale structures and external structures[4) - 9)] are proceeding.

The Tohoku Earthquake Disaster Report notes that adjacent areas, such as roadways and sidewalks, experienced substantially different degrees of damage[10)]. This shows the possibility that liquefaction damage can be greatly reduced by measures around the surface layer. In the first part of the current study, we clarify the state of the ground immediately below a structure which was tilted by liquefaction. Based on the results, we proposed a new liquefaction countermeasure by which the area immediately beneath the circumference of the foundations was replaced by gravel. Centrifugal model experiments were conducted, and the results confirmed that this greatly reduced tilting of the structure due to liquefaction.

2. STATUS OF THE GROUND BENEATH A STRUCTURE TILTED BY LIQUEFACTION

The condition of the ground under a structure tilted by liquefaction was investigated using centrifugal model experiments[11)]. As shown in Fig. 1, an eccentrically-loaded structure model was placed on a saturated ground with equally spaced layers of colored sand, and a shaking experiment was performed. The input was a sinusoidal wave with a frequency of 2 Hz and a maximum acceleration 300 cm/s^2 in actual scale. The input consists of 100 gradually increasing waves, 60 stationary waves, 5 gradually decreasing waves. The excitation time was 82.5 seconds in actual scale. Fig. 2 shows the increment of the inclination angle of the structure from the end of the excitation. This inclination angle increased slowly until 1,500 seconds, when the water pressure near the surface began to decrease even after the end of the excitation. Ultimately, the residual inclination angle of the structure was about 0.1 rad (≒ 1/10). After the experiment, the ground under the structure was cut in the vertical direction and observed.

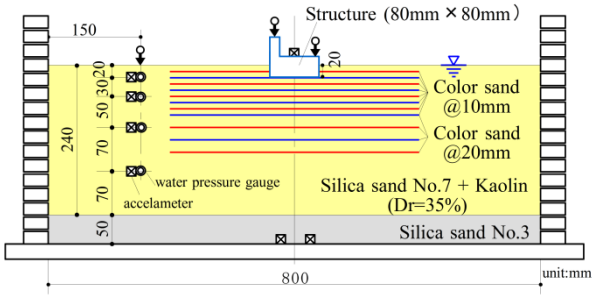

Fig. 1 Experiment model

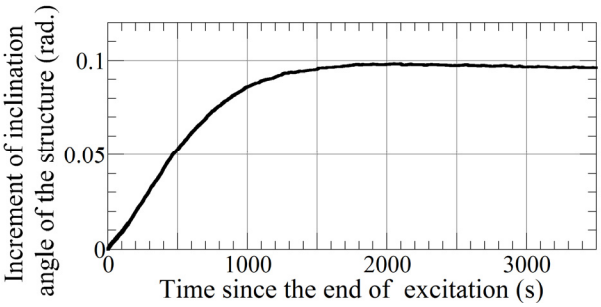

Fig. 2 Increment of inclination angle of the structure since the end of excitation

The condition of the structure after the experiment is shown as Photo 1, and the cross section of the ground beneath it is shown as Photo 2. The white area around the foundation in Photo 1 is kaolin clay accumulated from the ground material by sand boiling.

In Photo 2, the bands of colored sand remain distinct, demonstrating that no liquid-like mixing took place, even when the ground was liquefied, and little overall disturbance was produced. On the other hand, there were some places where the continuity of colored sand was broken just under the foundation's end where settlement was larger. This demonstrated that, even when liquefaction was induced, a clear shear surface (sliding surface) was generated from the base end in a manner similar to the centrifugal model experiment of the spread foundation performed using dry sand[12)] (Photo 3 and Fig. 3).

As it was impossible to install a camera to monitor the area surrounding the foundations, the exact relationship between the degree of tilting of the structure and boiling of the sand could not be clarified. However, as can be seen from Photo 2, on the side where settlement was smaller (the right-hand side of the photograph), the ground thickness shallower than the foundation's bottom (2nd

line) remained at its initial embedding depth. On the other hand, on the side where the settlement of the foundation was larger (the left-hand side of the photo), the thickness of the ground above the second line was thicker. Since the only large disturbance in the sand layers was observed at the shear surface, the kaolin clay that appeared around the foundation was assumed to originate mainly from this surface. Traces of sand boiling were observed also at positions away from the foundation. The depth of the ground disturbance due to sand boiling was about 1 cm. This suggests that these traces of sand boiling had little influence on tilting of the structure.

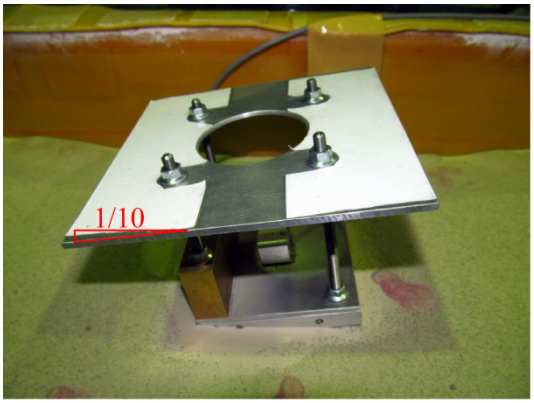

Photo 1 Structure model after experiment

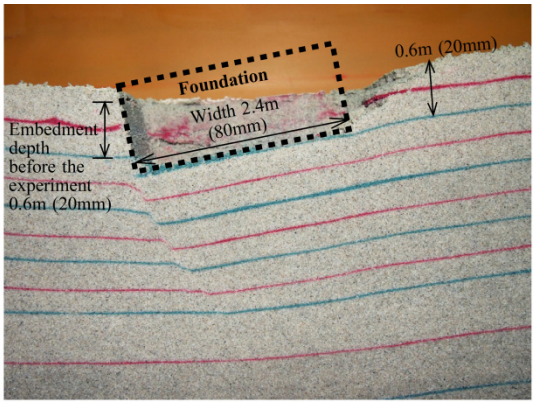

Photo 2 Cross section of the ground under the structure

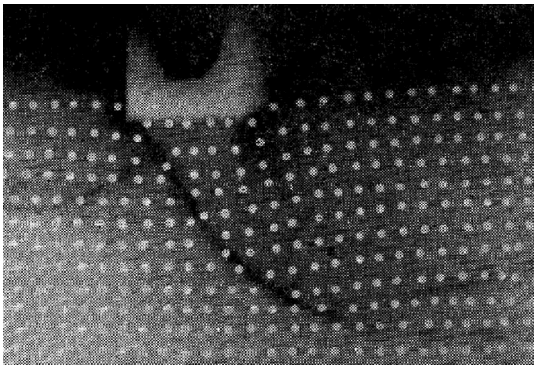

Photo 3 Shear surface generated under the foundation on dry sand[12)]

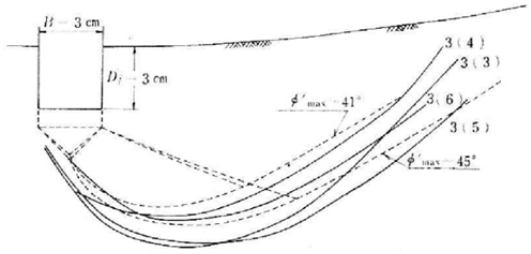

Fig.3 Shear surface generated under the foundation embedded in dry sand[12)]

3. A LIQUEFACTION COUNTERMEASURE FOR SMALL-SCALE STRUCTURES

The results reported in the previous section suggested that the damage caused by liquefaction could be significantly reduced by suppressing the development of a sliding surface, and that this could be achieved by improving the ground under the foundation circumference, which is the sliding surface's starting point. If a highly rigid material such as cement were to be used for soil improvement, a sliding surface may still form from the circumference of the improved area, and the inclination of the structure may not be suppressed[13)].

For this reason, we instead proposed the countermeasure shown in Fig. 4 (a), in which gravel-filled trenches with high water permeability are placed under the perimeter of the foundation. In an existing structure, the same effect can be achieved by adding gravel-filled trenches around the perimeter and extending the existing foundation. This is shown in Fig. 4 (b). By draining only the water from the gravel-filled trenches, liquefaction in these areas can be prevented. The trenches retain their rigidity and strength, and the formation of the sliding surface is suppressed. Although settlement caused by liquefaction in the deep ground still occurs, the inclination of the structure can be reduced

considerably.

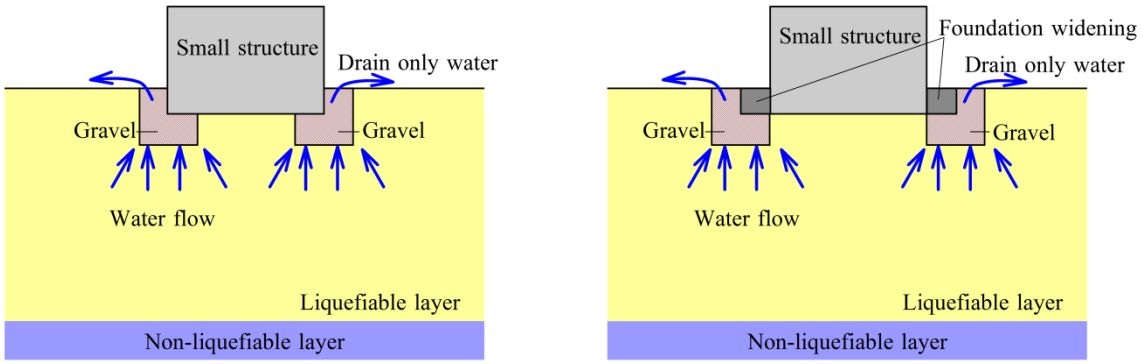

(a) Countermeasures for newly constructed structures (b) Countermeasures for existing structures

Fig. 4 Proposed liquefaction countermeasures for small structures

4. TESTING DAMAGE REDUCTION: CENTRIFUGAL MODEL EXPERIMENTS

4.1 Outline of experiments

Centrifugal model experiments were conducted to investigate the effect of the proposed countermeasures[14]. The experimental model is shown in Fig. 5. Experiments were performed at a centrifugal acceleration of 30g. A laminar share box with an inner length of 800 mm, width of 470 mm, and height of 370 mm was used. A 50 mm layer of silica No. 3 sand (D_{50} = 2.1 mm) was placed at the bottom of the box, and a liquefiable layer of thickness 240 mm (representing 7.2 m at the prototype scale) was created using a mix of silica No. 7 sand (D_{50}=0.33 mm) with 5% kaolin clay. The liquefiable layer was made with a relative density of 35%. To test the robustness of the proposed countermeasure, experiments were performed under more severe conditions than experienced in reality. Even at landfill sites, the relative density has been reported to be approximately 50 to 60%[15], and previous studies suggest that the shear strain at liquefaction becomes severe when the relative density is 40% or less[16]. The liquefiable layer was therefore given a relative density of 35%. The addition of kaolin clay reduced water permeability, thereby ensuring that the liquefied state was sustained over a long period. The physical constants of the sands are presented in Table 1 and the grain size accumulation curves are shown in Fig. 6. The permeability coefficient of silica No. 7 sand is 5.58×10^{-3} cm/s. The additional 5 % of kaolin clay reduces the permeability to approximately 43 %. The

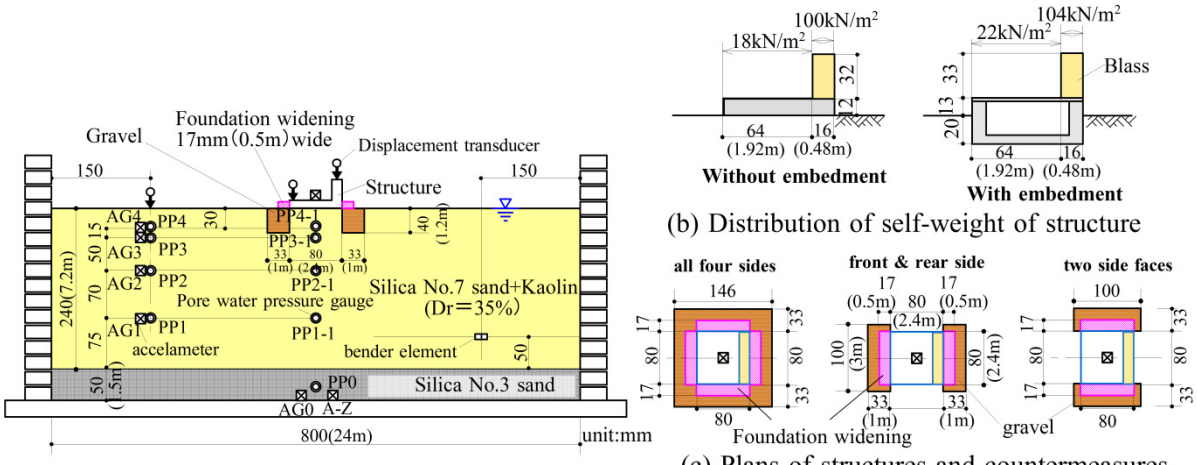

(a) Section

(b) Distribution of self-weight of structure

(c) Plans of structures and countermeasures

Fig. 5 Experiment model ( ): at prototype scale

similarity rule is shown in Table 2. Silicone oil with a specific gravity equal to that of water but a viscosity 30 times greater was used as a pore fluid to satisfy the similarity law for the diffusion process of water in soil. The S-wave velocity of the ground was measured during the process of increasing the centrifugal acceleration using the bender elements installed in the ground. Fig. 7 shows the relationship between the effective overburden pressure and the S-wave velocity in the liquefiable layer. The S-wave velocity from the ground surface to a ground layer of -2 m (where the effective overburden pressure was 16 kN/m^2) was between 50 and 100 m/s.

Table 1 Physical properties of soil

Soil	Silica No.7 sand + kaolin clay 5%	Silica No.3sand
Soil particle density	2.630 g/cm^3	2.654 g/cm^3
maximum dry density	1.599 g/cm^3	1.592$^{*)}$ g/cm^3
minimum dry density	1.206 g/cm^3	1.331$^{*)}$ g/cm^3
uniformity coefficient	4.77	1.63
coefficient of permeability	2.40×10^{-3} cm/s	4.77×10^{-1} cm/s

*) Not a formal test result because the particle size is large

Table 2 Similarity law of experiments

	Similarity rate
Length	1/N
Density	1
Stress	1
Pore water pressure	1
Displacement	1/N
Acceleration	N
Time	1/N
Time (permeability)	1/N^2

N:centrifugal acceleration

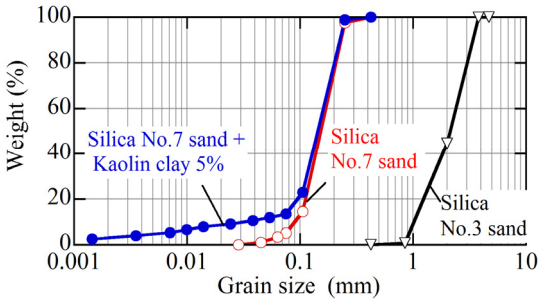

Fig. 6 Grain size accumulation curve of soil

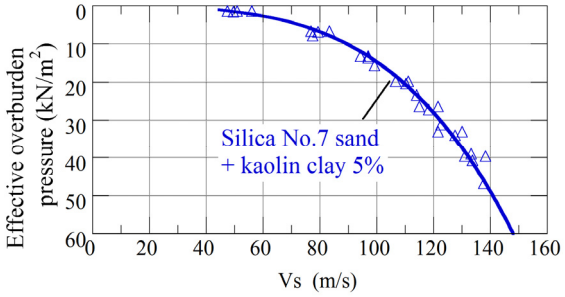

Fig. 7 Relationship between the effective overburden pressure and the S-wave velocity

Structure Model

The structure model shown in Figs. 5 (b) and (c) was fabricated from aluminum with an 80-mm square flat surface (equivalent to 2.4 m at a prototype scale) and a foundational thickness of 12 mm (0.36 m at prototype scale). A brass block with a width 20% that of the foundation was installed at one side, to impose an eccentric load and encourage tilting. To increase friction at the lower surface of the foundation, silica No. 7 sand was pasted on it using an adhesive. The contact pressure under centrifugal acceleration was approximately 100 kN/m^2 at the brass block part and approximately 18 kN/m^2 elsewhere, for an average value 34 kN/m^2.

The embedded foundation was replaced by a hollow aluminum member with a thickness of 33 mm (1m at prototype scale), and an embedded depth of 20 mm (0.6 m at prototype scale). The contact pressure in the embedded foundation was 104 kN/m^2 in the area under eccentric loading, 22 kN/m^2 elsewhere, and 38 kN/m^2 on average. Two structural models were arranged in a box to allow comparison of the results under different conditions. In order to reduce tilting of the structure by centrifugal loading, loadings up to 30g were investigated without load eccentricity by adding a counterweight. Once the centrifugal acceleration was unloaded, the counterweight was removed. The centrifugal acceleration was raised again up to 30g and a shaking-table test was performed. Therefore, at the time of the shaking-table tests, the ground under the structure was slightly over-consolidated.

Input Wave

A 2-Hz sine wave representing a maximum acceleration of 300 cm/s^2 at prototype scale was used as an input wave. The input seismic waveform is shown in Fig. 8. The input waveform is the same as that used in the experiment reported in Section 2.

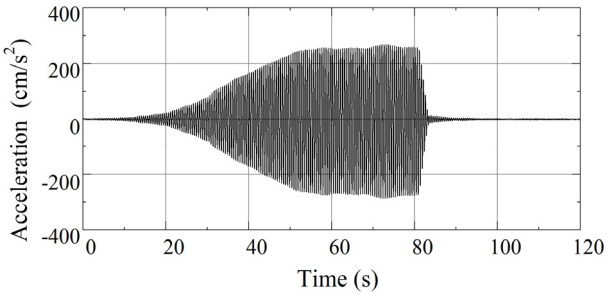

Fig. 8 Input seismic waveform

Countermeasures and Test Cases

The countermeasures used in the experiments included making gravel-filled trenches at the circumference of the foundation and widening the foundation altogether. The gravel used silica No. 3 sand. When gravel columns were used, they were 11 mm in diameter (330mm at prototype scale) and 40 mm in length (1.2 m at prototype scale). Three columns were made at each side of the foundation, at a spacing of 33 mm (1 m at prototype scale). A 10-mm layer of Silica No. 3 sand (0.3 m at prototype scale) was placed on the columns.

The foundation was extended 17 mm (0.51 m at prototype scale), i.e., approximately half of the trench width. As shown in Fig. 5(c), three configurations were tested: application to all four sides of the foundation, to the front (eccentric loading) and rear faces only, and to the two side faces only. The experimental cases are shown in Table 3.

Table 3 Experimental cases

Case	Embedment	Countermeasure direction	Gravel-filled trench
N0	—	—	—
N4-1.2	—	All sides	width 1m, depth 1.2m
NFB-1.2		Front & rear faces	width 1m, depth 1.2m
NLR-0.6		Two side faces	width 1m, depth 0.6m
NLR-1.2			width 1m, depth 1.2m
E0	0.6m	—	—
EFB-1.2D		Front & rear faces	width 1m, depth 0.3m + 3 gravel columns on each side (φ0.33m,1.2m length)

4.2 Test results

All data presented in following section are at prototype scale.

Pore water pressure

Figure 9 shows the time histories of the input acceleration (a), the response acceleration of the structure (b) , the pore water pressure and the excess pore water pressure ratio at G.L.-0.9 m (c, d) and those at G.L.-2.85 m (e, f) in Cases NLR-1.2, NFB-1.2, and N0 (no countermeasures). Cases NLR-1.2 and NFB-1.2 took place in the same laminar box. The pore water pressure of the ground on the portion where the structure was not placed (hereinafter referred to as the external ground) shows only the results of Cases NLR -1.2 and NFB-1.2. In Case N0, the result was almost the same. The graph of pore

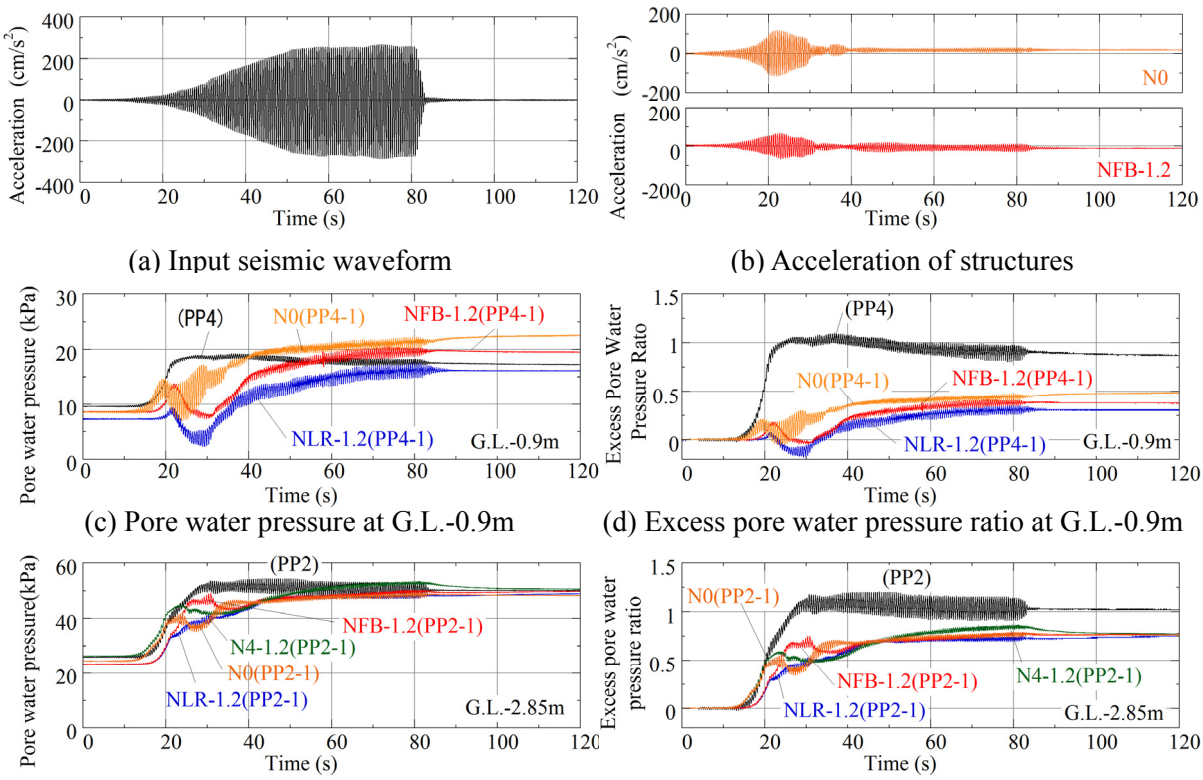

Fig. 9 Time histories of acceleration, pore water pressure and excess pore water pressure ratio

water pressure at G.L. -2.85 m also includes the results for Case N4-1.2. When calculating the excess pore water pressure ratio under the structure, the stress due to the structure's weight was taken into account.

The excitation time was 82.5 seconds, but the response acceleration of the structure decreased from around 23 seconds regardless of whether countermeasures were applied. After 30 seconds, the ground was estimated to have liquefied as the response acceleration was very small.

The pore water pressure under the structure (PP4-1, PP2-1) temporarily decreased, due to the shear strain associated with the inclination of the structure during excitation. At the end of the excitation period, however, the pore water paressure under the strucure was equal to or slightly greater than that in the external ground at all depths. Fig. 10 shows the results when a gravel layer with a thickness of 1.2 m underpinned the entire lower surface of the structure[13]. The rise in water pressure in the gravel portion was minimal, suggesting that the area replaced by gravel had high water permeability. In Fig. 9, when only the outer perimeter of the foundation was replaced by gravel, the

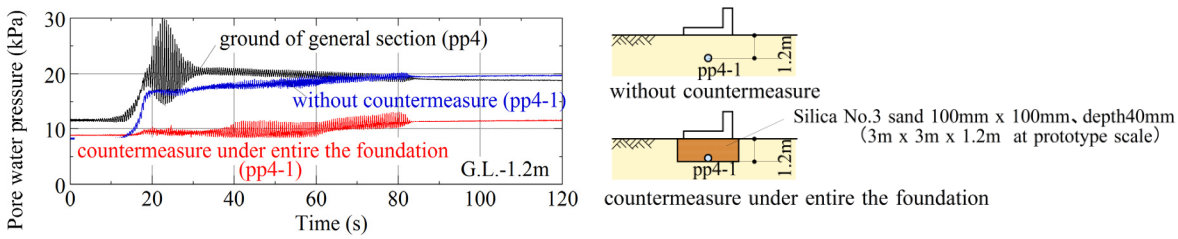

Fig. 10 Time histories of pore water pressure when the silica No. 3 sand is laid on the entire lower surface of the structure

rise in pore water pressure under the center of the foundation was not expected to be suppressed. At G.L.-2.85 m, deeper than the gravel bottom (G.L.-1.2 m), the pore water pressure rose by almost the same amount as in the external ground, even when countermeasures were applied. This confirmed that the countermeasures had little influence upon the rise in water pressure in the deeper ground. The excess pore water pressure ratio beneath the structure was below 1, regardless of whether countermeasures were applied.

Figure 11 shows the dissipation of the excess pore water pressure after excitation in Cases NLR-1.2, NFB-1.2, and N0. Since the kaolin clay was mixed to reduce the permeability, the liquefied state in the surface layer was maintained for about 1,200 seconds (Fig. 11 (a), (b)). In the process of increasing the pore water pressure, no significant difference was observed between the external ground and the ground beneath the structure (Fig. 9). When countermeasures were applied, the pore water pressure beneath the structure began to decrease at about 300 to 500 seconds. In the process of pore water pressure dissipation, the countermeasures were effective beneath the center of the structure. In contrast, in Case N0 (no countermeasures), the pore water pressure under the structure is slower to dissipate than in the external ground (Fig. 11 (a), (c)). This was due to the fact that at the end of the excitation, the water pressure of the ground under the structure becomes larger than that of the external ground due to the structure's weight. Thus, pore water pressure dissipation occurred so as to eliminate the water pressure difference between the ground under the structure and the external ground.

Settlement and Inclination of Structure

Figure 12 compares the time histories of structural settlement when countermeasures were and were not applied. The liquefaction duration in the surface layer is the time until the pore water pressure in the surface layer of the external ground (PP4) began to decrease (about 1,000 sec after the end of excitation in this case). In Case E0, the displacement transducer on the rear side deviated from the target at about 500 sec, making further measurement impossible. From the curve of the average settlement, most of the settlement occurred during excitation. The settlement increased slowly even after excitation ended. The average settlement during excitation was slightly larger when no countermeasures were applied, but the difference was not significant. After 1,000 sec, the excess pore water pressure ratio in the surface layer began to decrease, but the settlement of the structure slowly increased, taking 3,000 to 4,000 sec to complete. In the case without countermeasures (E0), the front side continued to settle and the rear side continued to rise after excitation ended, causing the inclination of the structure to increase further. In the case where countermeasures were taken (EFB-1.2D), both the front and rear of the structure settled by approximately the same amount after

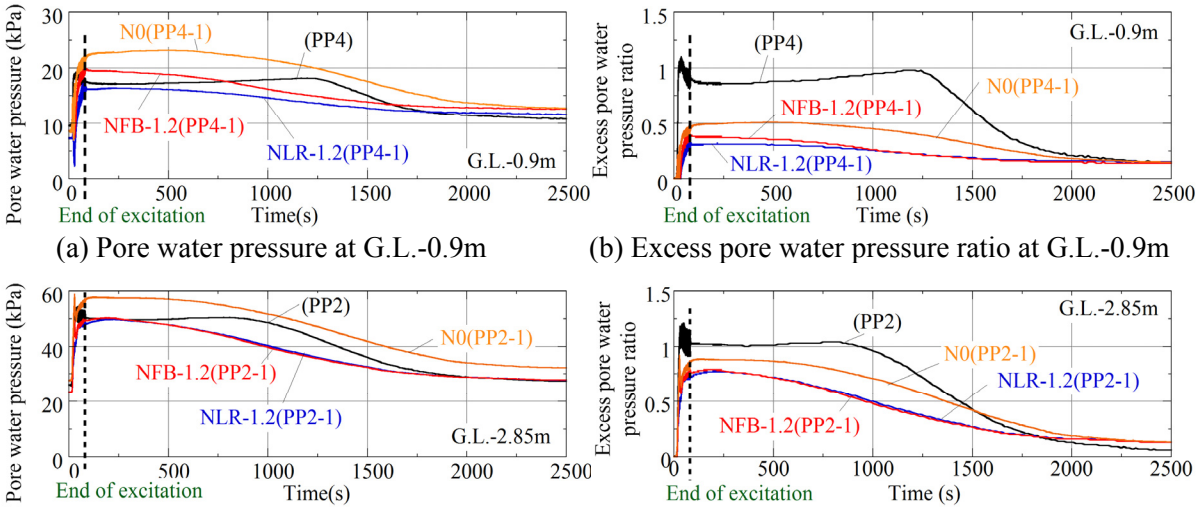

(a) Pore water pressure at G.L.-0.9m (b) Excess pore water pressure ratio at G.L.-0.9m

(c) Pore water pressure at G.L.-2.85m (d) Excess pore water pressure ratio at G.L.-2.85m

Fig. 11 Time histories in the pore water pressure dissipation process

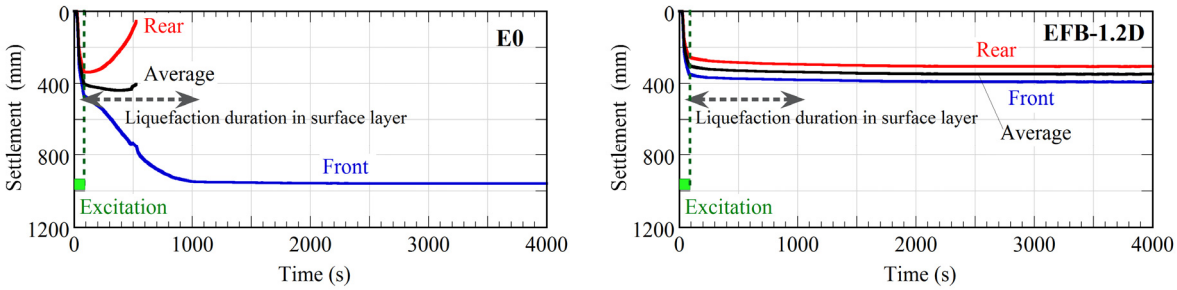

(a) E0 (without countermeasures) (b) EFB-1.2D

Fig. 12 Time histories of settlements of structures

excitation ended.

Figure 13 shows the increment of the inclination angle after the completion of excitation. If settlement on the side with an eccentric load was larger, the inclination angle was considered to be positive. In two cases without countermeasures (N0, E0), the inclination angles continued to increase, even after excitation ended, but almost halted when the excess pore water pressure in the surface layer of the external ground began to decrease. The large inclination in E0 caused the transducer on the rear side to become unmeasurable, such that the exact time at which inclination increase ended was not recorded. However, it was assumed to have also been at approximately 1,000 seconds, when the subsidence at the front of the structure ended (Fig.12). As shown in Fig. 9, the excess pore water pressure ratio under the structure remained below 1, even in Case N0 where no countermeasures were taken, but significant progressive inclination of the structure was observed. The increase in effective stress caused by the weight of the structure was small at the edge of the foundation. The effect of this stress in suppressing the generation of the slip surface shown in Photo 2 was assumed to be small.

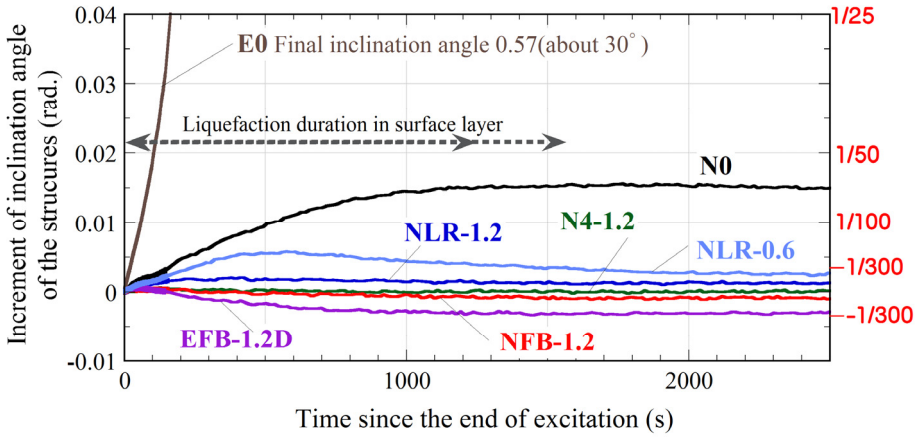

Fig. 13 Inclination increment of the structures after excitation

When no countermeasures were applied, the inclination angle of the embedded structure (E0) was larger than that of the non-embedded structure (N0). As can be seen from Fig. 14 (1), the foundation of the non-embedded structure was located on the ground surface, which is also the drainage surface. Although the excess pore water pressure generated beneath the foundation was dissipated at the perimeter, that generated outside the foundation attempted to dissipate to the closest ground surface. Figure 14 (2) shows that the boundary between the embedment of the foundation and the surrounding soil was more water-permeable than the external ground, because the sand faces the flat structure surface. Thus, in the embedment structure, the boundary between the embedment and the surrounding soil tends to be a water passageway. The edges of the foundation tend to act not only as drainage paths for the ground under the foundation, but also for the surrounding ground. This caused more water to be drained to the surface through the side of the embedment, and the amount of sand increased

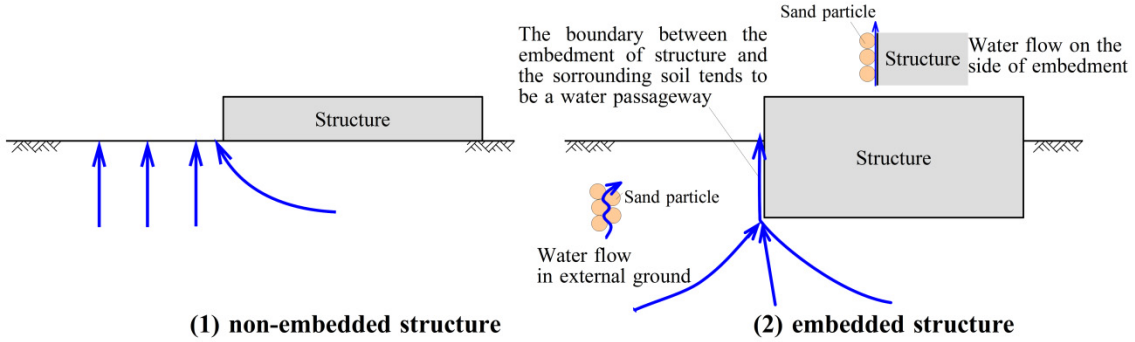

Fig. 14 Water flow during liquefaction with or without embedment

accordingly. It is inferred that the inclination angle of the structure became larger because the strength of the ground reduced due to reducing the density of the ground accompanying sand boiling.

In the case where countermeasures were applied at all four sides (N4-1.2), the increase in inclination angle of the structure after the end of excitation was close to zero, and in all cases to which countermeasures were applied, the final inclination angle was less than 1/300, even in the most extreme case (NLR-0.6). In these cases, inclination angle stopped increasing before the excess pore water pressure ratio in the surface layer of the external ground became less than 1. These results suggest that a large suppression effect can be expected even when countermeasures are applied only in two parallel directions on the perimeter of the foundation. As shown in Fig. 13, in Case NLR-0.6, the positive inclination (toward the eccentric load side) increased immediately after excitation ended but began to decrease after about 500 sec. This decrease was seen in almost all cases, even in the case without countermeasures (N0) after 2,000 sec. In Cases NFB-1.2 and EFB-1.2D, the positive inclination angle occurring during excitation (the settlement difference between the front and rear occurred before 100 sec in Fig. 12) decreased as soon as excitation ended; thus, it appeared that negative inclination angle occurred in Fig. 13. The decrease in the inclination angle of the structure was thought to be attributable to the following factors.

After liquefaction, the pore water pressure beneath the foundation almost equalized with that in the external ground due to seepage. This is shown in Figs. 9 and 11. Since the initial effective stress was smaller at the rear than that at the front, more excess pore water pressure needed to be dissipated. Therefore, dissipating the excess pore water pressure at the rear took longer than that at the front, so it is thought that halting settlement at the rear should also take longer. As no detailed measurements of the water pressure distribution in the ground were taken, elucidation of the mechanisms involved is left for future research.

Photo 4 shows the state of the model after completion of the experiment both with countermeasures (EFB-1.2D) and without (E0). The proposed countermeasures were shown to effectively suppress the inclination of the structure caused by liquefaction.

Photo 5 shows a cross section of the ground beneath the foundation post-experiment, from Case NFB-1.2. The gravel-filled trenches immediately under the foundation circumference preserved their initial shape.

5. CONCLUSIONS

We proposed a novel countermeasure against liquefaction damage for use in small structures. In this approach, the surface soil layer immediately under the perimeter of the foundation was replaced by gravel, opening a drainage route to the ground surface. Centrifugal model experiments were conducted to confirm the effectiveness of the proposed method, yielding the following conclusions.

1) Even when liquefaction was induced, a clear shear surface (sliding surface) was generated from the base end in a manner similar to the model experiment of the spread foundation performed using dry sand. The disturbance in other parts of the ground is relatively small.

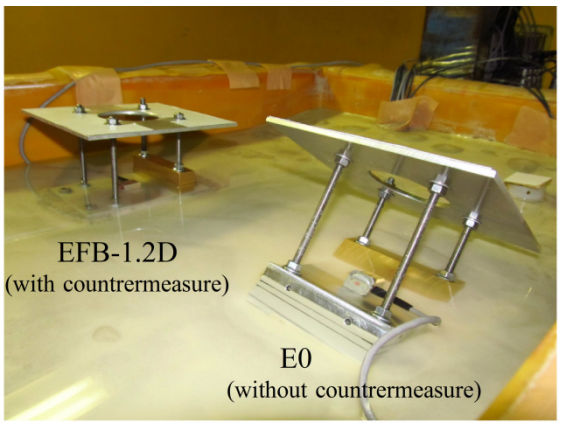

Photo 4 Status of structure models post-experiment

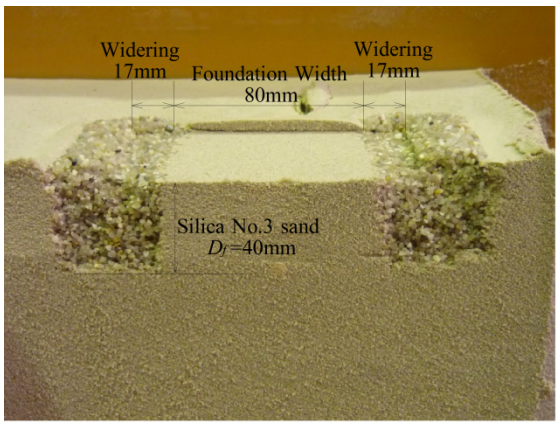

Photo 5 Cross section of the ground post-experiment (NFB-1.2)

2) Even when a large eccentric load is applied by establishing a gravel-filled trench 0.6–1.2-m deep immediately under the perimeter of the structure, the increment in inclination angle of the structure due to liquefaction remained below 1/300. This compares to inclination angles of between 1/70 and 1/2 when no countermeasures were applied, thus demonstrating that significant improvement could be achieved by applying countermeasures only in the surface layer.
3) With the exception of the gravel-filled trench and its immediate vicinity, the rise in water pressure was almost the same as when no countermeasures were applied, suggesting that liquefaction was not prevented. Therefore, although the inclination angle of the structure was decreased by the countermeasures, the average settlement was almost the same as that in the case without countermeasures.
4) To maximize suppression of inclination, countermeasures should be applied around the whole foundation. However, a significant reduction in tilting due to liquefaction was demonstrated even when countermeasures were applied only at two parallel sides.
5) When no countermeasures were applied, much greater tilting was observed when the structure was embedded. Even for the embedded structure, however, the proposed countermeasures achieved a large reduction the inclination due to liquefaction.

REFERENCES

1) For example, Kanto Regional Development Bureau, Ministry of Land, Infrastructure, Transportation and Tourism, Japanese Geotechnical Society: Report on the actual condition of ground liquefaction in the Kanto district due to The 2011 off the Pacific coast of Tohoku Earthquake, August, 2011 (in Japanese)
2) Harada, K., Obayashi, J. and Yoshitomi, H.: Verification of liquefaction measures by compaction method in buildings, The Foundation Eng. & Equipment, Vol.40, No.12, pp.47-49, 2012 (in Japanese)
3) Suzuki, Y., Saito, A., Onimaru, S., Kimura, T., Uchida, A. and Okumura, R.: Grid-shaped stabilized ground improved by deep cement mixing method against liquefaction for a building foundation, Soil mechanics and foundation engineering, Japanese Geotechnical Society, Vol.44, No.12, pp.47-49, 2012 (in Japanese).
4) Fukatsu, T., Sekiguchi, T., Nakai, S. and Mano, H.: Deterrent effect on liquefaction by lowering groundwater level in city block based on centrifuge shaking table test (Part1,2), Summaries of Technical Papers of Annual Meeting, Architectural Institute of Japan, B-1, pp.611-614, 2013 (in Japanese)
5) Suzuki, Y., Tokimatsu, K., Hidekawa, T. and Adachi, N.: Dynamic centrifuge model test of liquefaction countermeasures using both dewatering and drainage method foe existing houses (Part1-2), 48th Japan National Conf. on Geotech. Eng., pp.1603-1606, 2013 (in Japanese)

6) Akashi, T., Ohashi, M., Arai, H., Konishi, K., Tsukuni, S., Imai, M., Uchida, A. and Honda, T.: A study on the grid-form ground improvement as liquefaction countermeasure for existing small houses (Part1-3), 48th Japan National Conf. on Geotech. Eng., pp.1617-1622, 2013 (in Japanese)
7) Yasuda, S., Sasaki, S., Noguchi, C. and Ozawa, N.: Shaking table tests to study the possibility to prevent liquefaction-induced damage of houses by installing sheet piles (Part1-2), 48th Japan National Conf. on Geotech. Eng., pp.1759-1762, 2013 (in Japanese)
8) Nishiyama, T., Sahara, M. and Yamamoto, A.: Investigation of effects of shallow ground improvement for reducing structure settlement due to liquefaction, Summaries of Technical Papers of Annual Meeting, Architectural Institute of Japan, B-1, pp.631-632, 2013 (in Japanese)
9) Hirata, N., Takahashi, K., Miyata, K., Takaoka, Y., Obayashi, J., Harada, K., Suzuki, A, Yoshitomi, H., Hayashida, T. and Towhata, I.: Study on the construction method reducing liquefaction damage, 48th Japan National Conf. on Geotech. Eng., pp.1755-1756, 2013 (in Japanese)
10) Uchimura, T., Imamura, S., Kaneda, K., Onizuka, N., Koseki, J., Fujiwara, T., and Konishi, Y.: Organization and analysis of damaged information on public structures, Report meeting on research and examination of liquefaction and countermeasure technology in Urayasu city, three society association (JSCE, AIJ, JGS), 2012 (in Japanese)
11) Ishikawa, A., Yoshinari, K., Shamoto, Y. and Mano, H.: Observation of ground progressive failure due to liquefaction, 48th Japan National Conf. on Geotech. Eng., pp.1597-1598, 2013 (in Japanese)
12) Yamaguchi, H., Kimura, T. and Fujii, N.: Experimental studies on the bearing capacity of shallow foundations by the use of a centrifuge, Journal of JSCE, No.233, pp.71-85, 1975 (in Japanese)
13) Mano, H., Taji, Y., Shamoto, Y., Ishikawa, A. and Yoshinari, K.: Improvement method for progressive failure during and after liquefaction using by drainage (Part3-4), 47th Japan National Conf. on Geotech. Eng., pp.1387-1390, 2012 (in Japanese)
14) Mano, H., Shamoto, Y., Ishikawa, A. and Yoshinari, K.: Effect to reduce the liquefaction induced damage by drainage and widening the foundation (Part1-2), 48th Japan National Conf. on Geotech. Eng., pp.1599-1602, 2013 (in Japanese)
15) Shimizu, K. and Tohno, I.: Physical properties of reclamation soil in the Tokyo Bay area -Density characteristics-, 14th Japan National Conf. on Geotech. Eng., pp.181-184, 1979 (in Japanese)
16) Seed, H.B.: Soil liquefaction and cyclic mobility evaluation for level ground during earthquake, GED, ASCE, Vol.105, No.GT2, 1979, pp201-255.
17) Okamura, M., Takemura, J. and Ueno, K.: Centrifugal model test - Experimental technique and application to practical use- 2. Similarity law of centrifugal model test, Experimental technique, -Benefits and limitations, Soil mechanics and foundation engineering, Japanese Geotechnical Society, Vol.52, No.10, pp.37-44, 2004 (in Japanese)

(Original Japanese Paper Published: January, 2016)
(English Version Submitted: Jan 19, 2018)
(English Version Accepted: Feb 19, 2018)